Cardiovasc Intervent Radiol (2011) 34:139–148
DOI 10.1007/s00270-010-9987-7

LABORATORY INVESTIGATION

Self-Expanding Nitinol Renal Artery Stents: Comparison of Safety and Efficacy of Bare Versus Polyzene-F Nanocoated Stents in a Porcine Model

P. Kurz · U. Stampfl · P. Christoph · C. Henn · S. Satzl · B. Radeleff · I. Berger · G. M. Richter

Received: 7 December 2009 / Accepted: 26 August 2010 / Published online: 26 October 2010

Abstract
Objective To investigate the safety and efficacy of a Polyzene-F nanocoat on new low-profile self-expandable nitinol stents in minipig renal arteries.
Materials and Methods Ten bare nitinol stents (BNS) and 10 stents coated with a 50 nm-thin Polyzene-F coating were randomly implanted into renal arteries of 10 minipigs (4- and 12-week follow-up, 5 animals/group). Thrombogenicity, on-stent surface endothelialization, vessel wall injury, late in-stent stenosis, and peristrut vessel wall inflammation were determined by quantitative angiography and postmortem histomorphometry.
Results In 6 of 10 BNS, >50% stenosis was found, but no stenosis was found in stents with a nanothin Polyzene-F coating. Histomorphometry showed a statistically significant ($p < 0.05$) different average maximum luminal loss of 55.16% ± 8.43% at 12 weeks in BNS versus 39.77% ± 7.41% in stents with a nanothin Polyzene-F coating. Stents with a nanothin Polyzene-F coating had a significantly ($p < 0.05$) lower inflammation score after 12 weeks, 1.31 ± 1.17 versus 2.17 ± 0.85 in BNS. The results for vessel wall injury (0.6 ± 0.58 for Polyzene-F-coated stents; 0.72 ± 0.98 for BNS) and re-endothelialization, (1.16 ± 0.43 and 1.23 ± 0.54, respectively) were not statistically significant at 12-week follow-up. No thrombus deposition was observed on the stents at either follow-up time point.
Conclusion Nitinol stents with a nanothin Polyzene-F coating successfully decreased in-stent stenosis and vessel wall inflammation compared with BNS. Endothelialization and vessel wall injury were found to be equal. These studies warrant long-term pig studies (≥120 days) because 12 weeks may not be sufficient time for complete healing; thereafter, human studies may be warranted.

Keywords Interventional radiology · In-stent stenosis · Intimal hyperplasia · Nitinol · Renal artery stents · Polyzene-F

Introduction

The first published clinical experiences of renal artery stenting presented high technical success and 38% restenosis [1]. In-stent restenosis, occlusive overgrowth of neointimal tissue inside the stent, and worsening of renal function remain major concerns of renal artery stenting. In a meta-analysis of renal artery stenting studies, Leertouwer et al. described an average restenosis rate of 17% [2]. Worsening of renal function after stent placement has been reported as high as 5–18%, attributable to inadvertent plaque or cholesterol embolization, renal artery thrombosis during stent placement, or renal artery instrumentation in general [3–6]. Much progress has been made with respect to stent design, delivery systems, and implantation techniques, including minimizing the required catheter size, employing stent platforms, or applying embolic protection devices [7–12].

P. Kurz · G. M. Richter (✉)
Clinics for Diagnostic and Interventional Radiology, Klinikum Stuttgart, Kriegsbergstr. 60, 70174 Stuttgart, Germany
e-mail: g.richter@klinikum-stuttgart.de

I. Berger
Institute of General Pathology, Heidelberg, Germany

U. Stampfl · P. Christoph · C. Henn · S. Satzl · B. Radeleff
Department of Diagnostic and Interventional Radiology, University of Heidelberg, Heidelberg, Germany

The nitinol stent platform, a nickel (49.5–51%)-and-titanium-based thermoelastic alloy, achieved high acceptance for its shape-memory, marked crack-resistance behavior, and decrease of late in-stent stenosis compared with balloon-expandable stents in the superficial femoral artery [13–18]. When self-expandable stent delivery systems are used, renal artery morphology does not allow for easy passage across severe atherosclerotic lesions or precise stent implantation. To overcome this technical limitation, a small (5F) caliber stent delivery system for nitinol stents was designed and coated with a nanothin layer of Polyzene-F. The latter has proven to be effective in both decreasing early thrombogenicity and late in-stent stenosis in various animal models and in various arterial locations [19–24].

For the purpose of this study, a direct and side-by-side comparison minipig model was used to evaluate the safety and efficacy of a 5F-based nitinol stents with a nanothin Polyzene-F surface treatment versus bare nitinol stents (BNS). Primary study goals were to rule out thrombogenicity and in-stent stenosis. Secondary study goals were to investigate vessel wall injury and inflammation and on-stent surface endothelialization.

Materials and Methods

Stent and Polyzene-F Surface Treatment

Medical-grade nitinol stents were used, which had a length of 20 mm, an expanded bench diameter of 5.5 mm, and provided 10% to 20% renal artery overdilatation (Optimed; Karlsruhe, Germany). Stents had a sinusoidal design with strut arrangements and interstrut spacing similar to the previously tested balloon-expandable stents in several animal models [20–24]. A strut thickness of 210 μm was chosen to provide adequate resistance to hoop-stress and scaffolding forces. All stents were electropolished. To characterize resistance to hoop stress, the manufacturer compared the system with three other current self-expanding stent systems targeted at the same vascular dimension. The nanothin Polyzene-F surface-treatment technology has been previously described [20, 21]. In brief, the nanothin Polyzene-F surface treatment used in this study is ultrapure and has a molecular weight in excess of 10–25 $\times$ 10^6 g/mol. Bare metal nitinol stents were cleaned with acetone in an ultrasonic bath, dried, and subsequently exposed to a plasma-activation procedure. To ensure surface adhesion of Polyzene-F, the stents were covered by an adhesion promoter. Dip coating and subsequent solvent evaporation cycles were performed to achieve a 50-nm coating. High-resolution optical microscopy was then used to evaluate the presence of surface-coating defects on the nitinol stents. Two stents with a nanothin Polyzene-F coating were inspected with scanning electron microscopy (SEM) to confirm that stent surfaces were even and smooth; coating thickness was analyzed by ellipsometry and infrared spectroscopy; and the purity of the coating was confirmed by X-ray photoelectron spectroscopy. Before implantation, stents were assembled on the deployment system and ethylene-oxide sterilized (Optimed; Karlsruhe, Germany).

Animal Experiments

The study was designed and performed according to the guidelines and recommendations of the American Society of Laboratory Animal Practitioners [25]. Ten female Goettingen minipigs (Ellegard Minipigs Aps; Dalmose, Denmark), approximately 12 months old with a body weight from 17 to 22 kg, were used because previous animal experiments have shown swine in this size class have renal artery diameters of 4.5–5 mm [22]. Swine were divided into two groups: a 4-week postimplantation group and a 12-week postimplantation group. Stent implantation was performed by one investigator, who blinded to the type of the stent, and stents with a nanothin Polyzene-F coating and BNS were randomly assigned to either the right or left renal artery. For anaesthesia, the swine initially received an intramuscular injection consisting of ketamine 10 mg/kg (Ketanest S; Parke-Davis, Karlsruhe, Germany), azaperon 10 mg/kg (Stresnil; Janssen- Cilag GmbH, Neuss, Germany), and midazolam 1 mg/kg (Dormicum; Hoffmann-La Roche AG, Grenzach-Wyhlen, Germany). Anesthesia was then maintained by redosing of ketamine and midazolam as needed.

After surgically exposing the right femoral artery, the artery was punctured with a regular 3F puncture needle; a 10-cm 5F sheath was placed; and 2500 IU heparin were injected through the sidearm of the sheath. An aortic flush catheter was then introduced and advanced up to the proximal abdominal aorta. High-resolution abdominal angiography (Siemens Polystar Top; field of view 14 cm, 1024 $\times$ 1024 matrix) was performed. Right and left selective renal arteriograms were then obtained using a 4F selective angiographic catheter (Softouch Cobra 2 Curve; MeritMedical, South Jordan, UT). The stent delivery systems were advanced to the renal artery target site across a 0.020-inch gold-tipped guidewire. After stent deployment, the catheter was exchanged, and control angiography performed. The femoral artery was then sutured with Prolene 7.0 (Ethicon; Johnson & Johnson, New Brunswick, NJ) and the wound closed by applying routine surgical technique. No further anticoagulation or antiplatelet medication was administered throughout the follow-up intervals. Thus, the probability was increased for onset of early or late

thrombosis during evaluation of thrombogenicity, one of the secondary study goals.

Quantitative Angiographic Analysis

Before stent harvesting, renal angiograms were performed using the instrumentation described previously. However, the contralateral inguinal area was chosen as vascular entry site. Abdominal and renal angiograms were obtained through an aortic flush catheter placed at the ostia of the renal arteries. From the angiographic analysis, five quantitative variables were determined. Average stent diameter (STD) was determined using three in-stent angiographic reference points: the proximal third, middle third, and distal third of the stented area. In addition, the arterial segments immediately proximal and distal to the stented region were evaluated for possible arterial damage during stent deployment. The average luminal (in-stent) diameter (ALD) was evaluated at the previously mentioned locations using contrast-filled high-resolution follow-up angiograms. Minimal luminal diameter (MLD) was determined from the narrowest angiographic in-stent site at follow-up angiography. Late loss (LL), as the angiographic surrogate of late in-stent stenosis, was determined for each stent by subtracting ALD from STD. The value was expressed as absolute LL (mm) and as percentage late loss (%LL) related to the STD. Maximum late loss (MaxL) was calculated by subtracting MLD from STD and was expressed as absolute MaxL (mm) and as percentage MaxL (%MaxL).

A catagoric definition of late in-stent stenosis was based on the following dimensions: mild = maximum loss of diameter 10–30%; moderate = maximum loss of diameter 30–50%; and critical = maximum loss of diameter >50%. Angiographic presence of thrombus was presumed when a focal filling defect was observed within the stented area or its immediate adjacent vessel segments. The angiographic evaluations and assessments were performed by two members of the interventional team independently from the operator.

Stent Harvest

After completion of aortography, the aortic flush catheter was left in place with the side holes at the ostia of the renal artery. The abdominal wall was carefully opened, and ligation loops were placed around the aorta proximal and distal to the renal arteries. The loops around the aorta were then tightened, resulting in total aortic flow obstruction, at which time the swine intravenously received a lethal dose of ketamine (Ketanest S; Parke-Davis, Karlsruhe, Germany). On electrocardiogram indication of cardiac arrest, 1L saline was administered through the aortic catheter to rinse the arterial aortorenal compartment. In situ aortorenal pressure fixation was established through infusion of 500 ml buffered 4% formaldehyde at a pressure >100 mm Hg for at least 15 min and provided a fixed vessel dimension corresponding to the physiologic luminal character. Organs were surgically removed *en bloc* and immersed in buffered 4% formaldehyde for at least 1 week. Methylmethacrylate embedding (Technovit 9100; Heraeus, Kulzer GmbH & Co. KG, Wehrheim/Ts, Germany) was used for the stented arterial segments. The upstream and downstream portions of the methylmethacrylate cast-embedded specimens were separated with a diamond saw (Isomet; Buehler GmbH, Duesseldorf, Germany), and proximal, middle, and distal segments were prepared from each specimen. Each specimen had an initial thickness of 150–200 μm. They were then ground and polished (Minimet 1000; Buehler GmbH, Duesseldorf, Germany) to a final thickness of approximately 50 μm and stained with Toluidine blue. After staining, the specimens were photographed and digitalized (Picture It! 7.0; Microsoft, Redmond, WA). Optimas image analysis software version 6.0 (Optimas 6.0; Meyer Instruments, Houston, TX) was used for histomorphometry.

Quantitative Microscopy

Quantitative histomorphometery included analysis of neointimal height, stent strut injury score, and percentage stenosis according to Schwartz [26] and analysis of inflammation and endothelialization according to Kornowski [27]. Luminal area was characterized as the area circumscribed by the endothelial layer, the neointima as the area between the lumen and the internal elastic lamina (IEL), and the media as the area between the internal and external elastic lamina. Furthermore, the % stenosis ([1 − luminal area/IEL area] × 100) and the area of neointima (area of IEL − luminal area) were calculated. Neointimal thickness was determined by measuring the neointima layer on top of each visible stent strut. The medial thickness was determined as the medial layer measured behind each visible stent strut. In addition, the medial thickness was measured between stent struts. A standardized measuring lens was used for determination of endothelialization, injury, and inflammation scores.

Vessel injury caused by the stent struts was evaluated using the grade scale established by Schwartz [26]. In brief, grade 0 is characterized as an intact internal elastic lamina, denuded endothelium, and media compressed but not lacerated, and grade 3, the most severe, is characterized by a lacerated external elastic lamina and large lacerations of media extending through the external elastic lamina. An average injury score per stent was calculated from all struts of the proximal, middle, and distal segments.

Inflammation caused by the stent struts was characterized according to the Kornowski grading system [27]. In

brief, grade 0 is characterized by the absence of inflammatory cells surrounding the stent struts, and grade 3, the most severe, has circumferential dense lymphohistiocytic cell infiltration of the stent strut circumference. An average inflammation score per stent was calculated from all struts of the proximal, middle, and distal segments.

An endothelialization score was determined using the following grading system: grade 1 = continuous endothelial cell layer, grade 2 = noncontinuous endothelial cell layer, and grade 3 = no endothelial cells present on the stent. Again, an average endothelialization score per stent was calculated from all struts of the proximal, middle, and distal segments.

For all the above-mentioned assessments and determinations, a minimum of 5 and a maximum of 10 individual sites per specimen were chosen around its circumference to provide adequate quantification of the respective average per specimen. These histological evaluations was performed independently by two investigators with profound knowledge of vascular pathology and blinded to the type of the stent.

Statistical Analysis

Statview 5.0 (SAS; Chicago, IL) was used for descriptive and comparative statistical analyses of angiographic and microscopic measurement data. The nonparametric Wilcoxon ranked *t* test was applied for comparison of nonnormally distributed average neointimal heights, average percentage stenosis, average ALD, average STD, average %LL, and average %MaxL of stents with a nanothin Polyzene-F coating and BNS. All results were presented as means ± SDs. Fisher's exact test was applied for comparison of mild (<10%), moderate (<30%), and critical (>50%) stenosis, and $p < 0.05$ was considered statistically significant. These tests were recommended by the institutional consulting program of our university.

Results

Hoop Stress Comparison Test

As determined by the stent manufacturer's proprietary measurement system, the stent used for the study had a resistance to hoop stress of 87 mp/mm^2 before collapse. The other three stent types examined for comparsion had the following hoop-stress results: LifeStent (Bard) 98 mp/mm^2, Maris (Invatec) 71 mp/mm^2, and Everflex-Protege (ev3) 82 mp/mm^2. In contrast to the system tested for the study, the other three systems were based on 6F platforms.

Overall Procedural Success

No animals had to be withdrawn from the study because of implantation complications, and stents were placed at all target vasculature. Throughout respective follow-up intervals, all animals presented with good health until they were killed.

Thrombogenicity

No thrombus deposition was observed during angiography on either the stent with a nanothin Polyzene-F coating, the BNS, or adjacent arterial segments at the two follow-up intervals. This corresponded with the aforementioned uneventful clinical follow-up.

Quantitative Angiography and Histomorphometry

The quantitative angiography and histomorphometry results for stents with a nanothin Polyzene-F coating and for BNS are listed in Table 1. The diameter of the right renal artery before intervention was 4.6 ± 0.25 mm and that of the left was 4.7 ± 0.29 mm (not statistically significant). The diameters of the arteries after stent implantation measured between 5.1 and 5.3 mm, representing a desired overstretching of 10–20%. At 4 weeks after implantation, two stents with a nanothin Polyzene-F coating had <10% angiographic stenosis; three stents showed >30% stenosis; and no stent showed a critical stenosis. By contrast, one BNS had >10% stenosis, two had >30%; and two showed critical (binary) stenosis (>50%).

At 12 weeks, one stent with a nanothin Polyzene-F coating showed <10% stenosis, and the four remaining stents had <30% stenosis. In contrast, in the BNS group, one stent had a moderate and the other four stents a critical stenosis. This was statistically significant ($p < 0.01$). An example of a 12-week critical stenosis in a left renal artery after placement of a BNS is presented in Fig. 1, which shows virtually no restenosis on the Polyzene-F-coated stent on the right side.

Quantitative histomorphometry results were as follows: At 4 weeks after implantation, stents with a nanothin Polyzene-F coating had an average ALD of 3.97 ± 0.99 mm; an average STD 5.1 ± 0.16 mm, which corresponded to an average %LL of 22.05% ± 5.28%; and an average %MaxL of 37.19% ± 9.68%. These results are statistically significant ($p < 0.05$) compared with BNS, which had an average ALD of 3.28 ± 0.16 mm; an average STD of 5.3 ± 0.1 mm, which corresponded to an average %LL of 39.06 ± 22.72%; and an average %MaxL of 51.07% ± 25.13%.

At 12 weeks after implantation, stents with a nanothin Polyzene-F coating had an average ALD of 4.01 ±

Table 1 Quantitative angiographic analysis after 4 and 12 weeks after implantation[a]

	4 weeks after implantation			12 weeks after implantation		
	Polyzene-F ($n = 5$)	BNS ($n = 5$)	p[b]	Polyzene-F ($n = 5$)	BNS ($n = 5$)	p[b]
ALD (mm)	3.97 ± 0.99	3.28 ± 0.16	0.04	4.01 ± 1.14	2.89 ± 0.82	0.04
STD (mm)	5.1 ± 0.16	5.3 ± 0.15	0.04	5.5 ± 1.33	5.1 ± 1.15	0.04
LL (%)	22.05 ± 5.28	39.06 ± 22.72	0.04	28.89 ± 6.76	45.64 ± 6.77	0.04
MaxL (%)	37.189 ± 9.68	51.07 ± 25.13	0.04	39.77 ± 7.41	55.16 ± 8.43	0.04
Neointimal height (μm)	139.89 ± 14.78	442.17 ± 910.47	0.89	64.41 ± 78.73	492.86 ± 201.64	0.04
Stenosis (%)	31.4 ± 20.53	39.03 ± 33.59	0.34	23.21 ± 12.94	58.86 ± 14.97	0.04

ALD average luminal diameter, *STD* average stent diameter, *LL* average % late loss (STD-ALD), *MaxL* average maximum late loss (STD-MLD), *Stenosis* average % (1-luminal area (mm^2)/internal elastic lamina [mm])

[a] All values represent averages based on a minimum of 5 and a maximum of 10 individual measurements per specimen

[b] Calculated applying Wilcoxon signed rank test

Fig. 1 Critical stenosis (>50% luminal loss, ALD = 0.23 mm) demonstrated by quantitative angiography at 12 weeks in the left renal artery after placement of BNS. There is no restenosis on the coated stent shown on the right side (ALD = 0.48, % stenosis <10)

1.14 mm; an average STD of 5.5 ± 1.3 mm, which corresponded to an average %LL of 28.89% ± 6.76%; and an average %MaxL of 39.77% ± 7.41%. These results were statistically significant ($p < 0.05$) compared with BNS results. The average ALD of BNS was 2.89 ± 0.8 mm; the average STD was 5.06 ± 1.15 mm, which corresponded to an average %LL of 45.64% ± 6.76%; and an average %MaxL of 55.16% ± 8.43%. Analysis under light microscopy demonstrated a much greater extent of intimal hyperplasia on BNS compared with stents having a nanothin Polyzene-F coating at both 4 weeks and 12 weeks after implantation. At 4 weeks, the stents with a nanothin Polyzene-F coating had an average total neointimal height of 139.89 ± 148.78 μm and an average % stenosis of 31.4% ± 9.19%. Regarding BNS, the average neointimal height measured 442.17 ± 910.47 μm, and the average % stenosis was 39.03% ± 33.59%. At 12 weeks, the average neointimal height and % stenosis on stents with a nanothin Polyzene-F coating were significantly ($p < 0.05$) less than the average neointimal height and % stenosis on BNS. The stents with a nanothin Polyzene-F coating showed a low average neointimal height of 64.41 ± 78.7 μm and an accordingly low average % stenosis of 23.21% ± 12.94%. In the BNS, the average neointimal height was 492.86 ± 201.64 μm, and the average percentage stenosis was 58.86% ± 14.97%.

As seen in Fig. 2A, the vessel received a nitinol stent with a nanothin Polyzene-F coating and had minimal neointimal in-growth and grade 1 inflammation score. The vessel in Fig. 2B received a BNS and had mild stenosis and grade 2 inflammation. As seen in Fig. 2C, stents with a nanothin Polyzene-F coating had well-preserved vessel patency again at 12 weeks. Compared with the vessel in Fig. 2D, which received a BNS, critical stenosis and grade 3 inflammation occluded the vessel at 12 weeks.

Injury, Inflammation, and Endothelialization

The average injury score at 4 weeks after implantation was 1.06 ± 0.82 in stents with a nanothin Polyzene-F coating and 0.58 ± 0.48 in BNS. At 12 weeks, the average injury score was 0.6 ± 0.58 in stents with a nanothin Polyzene-F coating and 0.72 ± 0.98 in BNS. At both postimplantation intervals, there were extreme differences between the average inflammation score of stents with a nanothin Polyzene-F coating and that of BNS. The average inflammation score at 4 weeks after implantation for stents with a nanothin Polyzene-F coating was 0.29 ± 0.45 and was 0.87 ± 1.14 in BNS, more than three times greater than stents with a nanothin Polyzene-F coating ($p = 0.04$). The

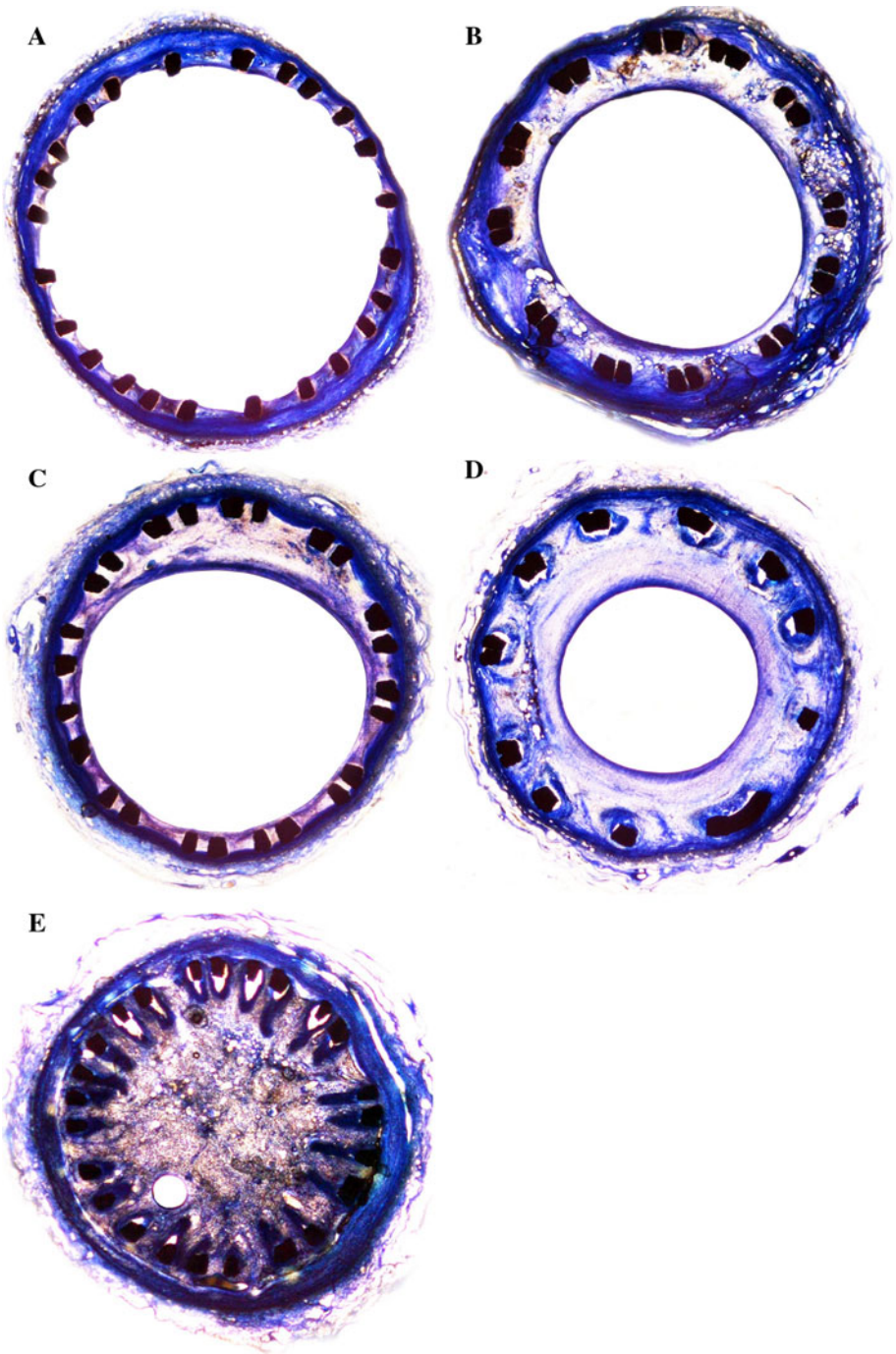

Fig. 2 **A** Photomicrograph of a stented vessel segment with a self self-expanding nitinol stent having a nanothin Polyzene-F coating at 4 weeks after implantation, stained with Toluidine blue, and imaged at 10× magnification of the original specimen. The average % stenosis was calculated as 12%. **B** Photomicrograph of a bare metal nitinol-stented vessel segment at 4 weeks after implantation, stained with Toluidine blue, and imaged at 10× magnification of the original specimen. The average % stenosis was calculated as 36%. **C** (same animal as in Fig. 1) Photomicrograph of the middle section of a self-expanding nitinol stent with a nanothin Polyzene-F coating at 12 weeks after implantation, stained with Toluidine blue, and imaged at 10× magnification of the original specimen. The average % stenosis was calculated as 17%. **D** Photomicrograph of the middle section of a bare metal nitinol stent at 12 weeks after implantation with a critical stenosis of >50 (average % stenosis 62%), stained with Toluidine blue, and imaged at 10× magnification of the original specimen. **E** (same animal as in Fig. 1) Photomicrograph of the middle section of a bare metal nitinol stent at 12 weeks after implantation with a severe stenosis and pronounced peristrut inflammation, stained with Toluidine blue, and imaged at 10× magnification of the original specimen. The average % stenosis was calculated as 92%

average inflammation score at 12 weeks for stents with a nanothin Polyzene-F coating at 1.31 ± 1.17 was significantly ($p < 0.02$) less than the average inflammation score of BNS at 2.17 ± 0.85. The endothelialization score for stents with a nanothin Polyzene-F coating at 4 weeks was 1.29 ± 0.45 and was 1.2 ± 0.41 for BNS. At 12 weeks, the scores were 1.16 ± 0.43 and 1.23 ± 0.54, respectively. These differences were not statistically significant.

Discussion

Since clinical introduction in the late 1980s [1], renal artery stenting has been accepted as a minimally invasive method to treat renal hypertension or renal failure resulting from renal artery stenosis. Renal artery stenting combines adequate long-term patency with clinical success [10, 12, 28]. Recent advances in catheter technology, including the low-profile (5F) delivery systems, have increased the interest in self-expandable nitinol stents for treatment of renal artery stenosis. In the superficial femoral artery, nitinol stent-based studies showed promising results with respect to decreasing neointimal hyperplasia and late in-stent stenosis. Specifically, in 2006, Schillinger et al. showed that self-expandable nitinol stents provided superior results compared with balloon angioplasty and stenting of the superficial femoral artery [15]. In addition, a 2-year follow-up of the patients receiving a self-expandable nitinol stent showed that they continued to have improved stent patency compared with the patients receiving angioplasty [16]. Verheye et al. showed, in a porcine carotid and iliac model, that nitinol stents appeared to have a favorable biocompatibility [29]. In the Sirocco trials, which compared sirolimus-eluting and bare metal long-segment nitinol stents in the superficial femoral artery, both the active and the passive stent versions had a low restenosis rate at 6 months [17] and at longer follow-up, which included a greater patient population [18]. Analyzing the results of our experimental study, the BNS, even in a modern low-profile design, failed to decrease late in-stent stenosis and inflammation in the chosen renal artery model. Specifically, at 12 weeks after implantation, the BNS showed disappointing results in almost every investigated aspect: angiographic binary stenosis, percentage stenosis, and inflammation. In the attempt to explain these negative findings, it is important to note that stent expansion or focal strut-induced vascular injury, which is considered as one of the most important trigger effects of excessive late in-stent stenosis [30–32], can be virtually ruled out as a contributing or causative factor because at both postimplantation time points, the injury scores were far lower than any critical value. Another conflicting result from the BNS group was the usual pattern of excessive intimal hyperplasia. At both intervals, endothelialization of the BNS surfaces was nearly complete. In this context, the most pertinent explanation for the overall negative findings of the BNS results from the excessive level of inflammation elicited by the stent struts. Kornowski suggested that inflammation plays an important role in neointimal formation after stenting and described significant correlations between the degree of inflammation and neointimal formation, measured either as neointimal height, neointimal area, or percentage stenosis [27]. Furthermore, he detected correlations between severe inflammatory reaction and perforation of the internal or external elastic membrane [27].

In the present study, almost each strut of the BNS at 12 weeks after implantation showed circumferential moderate or dense lymphohistiocytic cell infiltration, accounting for an average inflammation score of 2.17. Furthermore, these results are corroborated by the time course of inflammation, which was significantly lower at 4 weeks than at 12 weeks after implantation. The observed increase in peristrut inflammation virtually mirrors the time course of angiographic and microscopic in-stent stenosis or late loss, which also increased significantly with time in the BNS. It has been hypothesized that contact allergies, especially to nickel, triggered by metallic surfaces or ion release, induce inflammatory reactions associated with neointima hyperplasia and in-stent stenosis [33]. Wataha et al. indicated that the release of nickel ions poses a risk of promoting an inflammatory response in soft tissue by activating monocytes [34].

The neointimal height, percentage stenosis, and inflammation score of the self- expanding nitinol stents with a nanothin Polyzene-F coating suggests that this coating technology can decrease the cellular events related to in-stent restenosis of stents used in renal arteries. Furthermore, no on-stent or in-segment thrombus was detected in stents having a nanothin Polyzene-F coating neither at angiography nor at light microscopy. Welle and Grunze described the potential of Poly(Bis(Trifluoroethoxy))Phosphazene (PTFEP) to serve as a thromboresistant coating based on the selective absorption of albumin, which is known to decrease platelet apposition, and decreased fibrinogen absorption compared with carbon-based coating materials [35]. These properties have been confirmed *ex vivo* and in various animal models: Richter et al. confirmed the thromboresistant potential of Polyzene-F using SEM in a rabbit iliac artery model, in which small-calibre stents with a nanothin Polyzene-F coating were completely free of any thrombus deposition at 1 week [20]. Moreover, with regard to the theoretically high probability of thrombus formation, the rabbits did not receive any antithrombotic or antiplatelet medication during the follow-up period. Low platelet and thrombus depositions on stents with a nanothin Polyzene-F coating might also contribute to the favorable angiographic outcome and known ability to

decrease neointimal formation as not only shown in renal but also porcine coronary artery models [20, 21, 23, 24].

The low level of angiographic in-stent stenosis of stents with a nanothin Polyzene-F coating was confirmed by quantitative histomorphometry. The average neointimal height decreased from approximately 140 μm at 4 weeks to 70 μm at 12 weeks, which indicated stabilization and maturization of neointima. Maturity and stability of the neointima is further supported by the high degree of endothelialization of stents with a nanothin Polyzene-F coating at 12 weeks (score of 1.1). Specifically, the low absolute neointimal height of 70 μm at 12 weeks compares favorably with other experimental bare metal stent versus coated stent studies [22]. For example, polytetrafluoroethylene (PTFE)-coated renal stents showed intimal heights of 350 μm at 12 weeks [36]; carbon-coated renal artery stents had an average neointimal height of 150 μm at 12 weeks [37]; and fibrin-coated coronary artery stents had an average neointimal height of 560 μm at 4 weeks [38].

Last, the relative high strut thickness of 210 μm, required for sufficient scaffolding stability of the nitinol stents, might have contributed to the negative outcome of the BMS [39]. In the stents with a nanothin Polyzene-F coating, the stent strut thickness may have been counteracted by the beneficial biologic effects of Polyzene-F. Strut geometry and stent design, especially strut thickness, have been identified as a potential factor for increased intimal hyperplasia, arterial thrombosis, and increased inflammatory long-term reaction [30, 40–45]. However, Garasic et al. suggested that variations in strut thickness between 125 and 200 μm have no significant impact on the investigated biologic end points, such as thrombogenicity [30]. This could explain why BNS were not associated with a higher risk of thrombogenicity but had excessive late in-stent stenosis. Several experimental and clinical studies have described the negative effects and arterial wall response of stent-induced wall overstretch and wall injury [30–32]. Vessel wall injury increases exponentially with stent deployment diameter, highlighting the importance of adequate stent overexpansion and novel stent designs that specifically address peak stress decrease [40]. Overexpansion or excessive vessel wall injury did not contribute to the negative results of the BNS results in this study. Therefore, strut thickness of 210 μm, in concert with the elicited inflammatory reaction, may have contributed to the high neointima in the BNS. Both experimentally and in clinical studies, a strong negative correlation between stent strut thickness and intimal hyperplasia has been shown [41–45].

Limitations of the Study

Although this study represents a standardized approach for direct side-to-side comparisons of nitinol stents, its applicability to human arteriosclerotic disease is limited because native arteries were used. The wall characteristics and biologic response pattern of these arteries is not completely reflected in humans. This native artery model was used instead of an atherosclerotic diet model to avoid bias from potential differences in disease burden at the implantation target. Furthermore, the number of animals, obviously, is limited and no antiplatelet or anticoagulant medication was given. Hence, a transfer into clinical reality might require further experimental and design studies focusing on the special characteristics of renal artery stenting. It is not known whether a different pattern of respiratory up and downward movement of the minipig arteries is existent and might cause a different "motion injury" pattern compared with the erect human being. Such, of course, is of relevance in interpreting our results with special focus to arterial injury and inflammation.

Conclusion

Although modern catheter technology allows the safe and precise placement of self-expanding nitinol stents, the biologic response to BNS proves to be unfavorable in the renal artery territory in striking contrast to the human superficial femoral artery. Technical success was achieved in 100% of the minipigs used in this study. However, the excessive and specific vessel wall reaction to the alloy itself is responsible for the poor long-term outcome, as expressed by the high level of peristrut inflammation, which increased with time. Accordingly, the favorable results of stents with a nanothin Polyzene-F surface treatment can be attributed to the thromboresistance and high biocompatibility of this polymer and near complete endothelialization as early as 4 weeks, which significantly ($p < 0.05$) surpassed that of BNS at 12 weeks. In summary, it can be concluded that a nitinol stent with a nanothin Polyzene-F coating was able to abolish the negative effects of the nitinol alloy when used in the renal arteries.

Conflict of interest Authors U. S. and G. M. R received a research grant from CeloNova Biosciences, Newnan, GA, and G. M. R. has served as a consultant to CeloNova Biosciences, Newnan, GA.

References

1. Rees CR, Palmaz JC, Becker GJ et al (1991) Palmaz stent in atherosclerotic stenoses involving the ostia of the renal arteries: preliminary report of a multicenter study. Radiology 181: 507–514
2. Leertouwer TC, Gussenhoven EJ, Bosch JL et al (2000) Stent placement for renal arterial stenosis: where do we stand? A meta-analysis. Radiology 216:78–85

3. Sivamurthy N, Surowiec SM, Culakova E et al (2004) Divergent outcomes after percutaneous therapy for symptomatic renal artery stenosis. J Vasc Surg 39:565–574
4. Ahmadi R, Schillinger M, Sabeti S et al (2002) Renal artery PTA and stent implantation: immediate and late clinical and morphological outcome. Wien Klin Wochenschr 114:21–27
5. Boisclair C, Therasse E, Oliva VL et al (1997) Treatment of renal angioplasty failure by percutaneous renal artery stenting with Palmaz stents: midterm technical and clinical results. AJR Am J Roentgenol 168:245–251
6. Gill KS, Fowler RC (2003) Atherosclerotic renal arterial stenosis: clinical outcomes of stent placement for hypertension and renal failure. Radiology 226:821–826
7. Chade AR (2006) Revascularization in atherosclerotic renovascular disease: problems beyond the obstruction. Kidney Int 70: 830–832
8. Holden A, Hill A, Jaff MR, Pilmore H (2006) Renal artery stent revascularization with embolic protection in patients with ischemic nephropathy. Kidney Int 70:948–955
9. Holden A, Hill A (2003) Renal angioplasty and stenting with distal protection of the main renal artery in ischemic nephropathy: early experience. J Vasc Surg 38:962–968
10. Muller-Hulsbeck S, Frahm C, Behm C et al (2005) Low-profile stent placement with the monorail technique for treatment of renal artery stenosis: midterm results of a prospective trial. J Vasc Interv Radiol 16:963–971
11. Neumann C, Gschwendtner M, Karnel F, Mair J, Dorffner G, Dorffner R (2005) Technical feasibility of the implantation of a monorail stent system into the renal arteries without pre-dilatation. Rofo 177:84–88
12. Amighi J, Sabeti S, Dick P et al (2005) Impact of the rapid-exchange versus over-the-wire technique on procedural complications of renal artery angioplasty. J Endovasc Ther 12:233–239
13. McKelvey AL, Ritchie RO (1999) Fatigue-crack propagation in Nitinol, a shape-memory and superelastic endovascular stent material. J Biomed Mater Res 47:301–308
14. Robertson SW, Ritchie RO (2007) In vitro fatigue-crack growth and fracture toughness behavior of thin-walled superelastic Nitinol tube for endovascular stents: a basis for defining the effect of crack-like defects. Biomaterials 28:700–709
15. Schillinger M, Sabeti S, Loewe C et al (2006) Balloon angioplasty versus implantation of nitinol stents in the superficial femoral artery. N Engl J Med 354:1879–1888
16. Schillinger M, Sabeti S, Dick P et al (2007) Sustained benefit at 2 years of primary femoropopliteal stenting compared with balloon angioplasty with optional stenting. Circulation 115: 2745–2749
17. Duda SH, Pusich B, Richter G et al (2002) Sirolimus-eluting stents for the treatment of obstructive superficial femoral artery disease: six-month results. Circulation 106:1505–1509
18. Duda SH, Bosiers M, Lammer J et al (2005) Sirolimus-eluting versus bare nitinol stent for obstructive superficial femoral artery disease: the SIROCCO II trial. J Vasc Interv Radiol 16:331–338
19. Huang Y, Liu X, Wang L, Li S, Verbeken E, De Scheerder I (2003) Long-term biocompatibility evaluation of a novel polymer-coated stent in a porcine coronary stent model. Coron Artery Dis 14:401–408
20. Richter GM, Stampfl U, Stampfl S et al (2005) A new polymer concept for coating of vascular stents using PTFEP (poly(bis(trifluoroethoxy)phosphazene) to reduce thrombogenicity and late in-stent stenosis. Invest Radiol 40:210–218
21. Satzl S, Henn C, Christoph P et al (2007) The efficacy of nanoscale poly[bis(trifluoroethoxy) phosphazene] (PTFEP) coatings in reducing thrombogenicity and late in-stent stenosis in a porcine coronary artery model. Invest Radiol 42:303–311
22. Henn C, Satzl S, Christoph P et al (2008) Efficacy of a polyphosphazene nanocoat in reducing thrombogenicity, in-stent stenosis, and inflammatory response in porcine renal and iliac artery stents. J Vasc Interv Radiol 19:427–437
23. Stampfl U, Sommer CM, Thierjung H et al (2008) Reduction of late in-stent stenosis in a porcine coronary artery model by cobalt chromium stents with a nanocoat of polyphosphazene (Polyzene-F). Cardiovasc Intervent Radiol 31:1184–1192
24. Radeleff B, Thierjung H, Stampfl U et al (2008) Restenosis of the CYPHER-Select, TAXUS-Express, and Polyzene-F nanocoated cobalt-chromium stents in the minipig coronary artery model. Cardiovasc Intervent Radiol 31:971–980
25. Brown MJ, Pearson PT, Tomson FN (1993) Guidelines for animal surgery in research and teaching. AVMA Panel on Animal Surgery in Research and Teaching, and the ASLAP (American Society of Laboratory Animal Practitioners). Am J Vet Res 54:1544–1559
26. Schwartz CJ, Sprague EA, Valente AJ, Kelley JL, Edwards EH (1989) Cellular mechanisms in the response of the arterial wall to injury and repair. Toxicol Pathol 17:66–71
27. Kornowski R, Hong MK, Tio FO, Bramwell O, Wu H, Leon MB (1998) In-stent restenosis: contributions of inflammatory responses and arterial injury to neointimal hyperplasia. J Am Coll Cardiol 31:224–230
28. Knipp BS, Dimick JB, Eliason JL et al (2004) Diffusion of new technology for the treatment of renovascular hypertension in the United States: surgical revascularization versus catheter-based therapy, 1988–2001. J Vasc Surg 40:717–723
29. Verheye S, Salame MY, Robinson KA et al (1999) Short- and long-term histopathologic evaluation of stenting using a self-expanding nitinol stent in pig carotid and iliac arteries. Catheter Cardiovasc Interv 48:316–323
30. Garasic JM, Edelman ER, Squire JC, Seifert P, Williams MS, Rogers C (2000) Stent and artery geometry determine intimal thickening independent of arterial injury. Circulation 101: 812–818
31. Leopold JA, Loscalzo J (2000) Clinical importance of understanding vascular biology. Cardiol Rev 8:115–123
32. Schwartz RS, Huber KC, Murphy JG et al (1992) Restenosis and the proportional neointimal response to coronary artery injury: results in a porcine model. J Am Coll Cardiol 19:267–274
33. Koster R, Vieluf D, Kiehn M et al (2000) Nickel and molybdenum contact allergies in patients with coronary in-stent restenosis. Lancet 356:1895–1897
34. Wataha JC, Lockwood PE, Marek M, Ghazi M (1999) Ability of Ni-containing biomedical alloys to activate monocytes and endothelial cells in vitro. J Biomed Mater Res 45:251–257
35. Welle A, Grunze M, Tur D (1998) Plasma protein adsorption and platelet adhesion on poly. J Colloid Interface Sci 197:263–274
36. Sangiorgi G, Arbustini E, Lanzarini P et al (2001) Nonbiodegradable expanded polytetrafluoroethylene-covered stent implantation in porcine peripheral arteries: histologic evaluation of vascular wall response compared with uncoated stents. Cardiovasc Intervent Radiol 24:260–270
37. Galloni M, Prunotto M, Santarelli A et al (2003) Carbon-coated stents implanted in porcine iliac and renal arteries: histologic and histomorphometric study. J Vasc Interv Radiol 14:1053–1061
38. Holmes DR, Camrud AR, Jorgenson MA, Edwards WD, Schwartz RS (1994) Polymeric stenting in the porcine coronary artery model: differential outcome of exogenous fibrin sleeves versus polyurethane-coated stents. J Am Coll Cardiol 24: 525–531
39. Briguori C, Sarais C, Pagnotta P et al (2002) In-stent restenosis in small coronary arteries: impact of strut thickness. J Am Coll Cardiol 40:403–409

40. Ballyk PD (2006) Intramural stress increases exponentially with stent diameter: a stress threshold for neointimal hyperplasia. J Vasc Interv Radiol 17:1139–1145
41. Hara H, Nakamura M, Palmaz JC, Schwartz RS (2006) Role of stent design and coatings on restenosis and thrombosis. Adv Drug Deliv Rev 58:377–386
42. Sangiorgi G, Melzi G, Agostoni P et al (2007) Engineering aspects of stents design and their translation into clinical practice. Ann Ist Super Sanita 43:89–100
43. Palmaz JC, Bailey S, Marton D, Sprague E (2002) Influence of stent design and material composition on procedure outcome. J Vasc Surg 36:1031–1039
44. Rittersma SZ, de Winter RJ, Koch KT et al (2004) Impact of strut thickness on late luminal loss after coronary artery stent placement. Am J Cardiol 93:477–480
45. Pache J, Kastrati A, Mehilli J et al (2003) Intracoronary stenting and angiographic results: strut thickness effect on restenosis outcome (ISAR-STEREO-2) trial. J Am Coll Cardiol 41:1283–1288